Inorganic Chemistry

Article

pubs.acs.org/IC

Metal–Organic Framework Nanocrystals as Sacrificial Templates for Hollow and Exceptionally Porous Titania and Composite Materials

Hui Yang,*[,†] Paul E. Kruger,*[,‡] and Shane G. Telfer*[,†]

[†]MacDiarmid Institute for Advanced Materials and Nanotechnology, Institute of Fundamental Sciences, Massey University, Palmerston North 4442, New Zealand

[‡]MacDiarmid Institute for Advanced Materials and Nanotechnology, Department of Chemistry, University of Canterbury, Christchurch 8140, New Zealand

Supporting Information

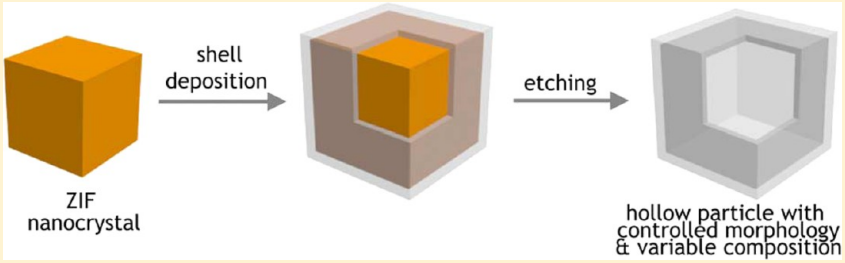

ABSTRACT: We report a strategy that employs metal–organic framework (MOF) crystals in two roles for the fabrication of hollow nanomaterials. In the first role the MOF crystals provide a template on which a shell of material can be deposited. Etching of the MOF produces a hollow structure with a predetermined size and morphology. In combination with this strategy, the MOF crystals, including guest molecules in their pores, can provide the components of a secondary material that is deposited inside the initially formed shell. We used this approach to develop a straightforward and reproducible method for constructing well-defined, nonspherical hollow and exceptionally porous titania and titania-based composite nanomaterials. Uniform hollow nanostructures of amorphous titania, which assume the cubic or polyhedral shape of the original template, are delivered using nano- and microsized ZIF-8 and ZIF-67 crystal templates. These materials exhibit outstanding textural properties including hierarchical pore structures and BET surface areas of up to 800 m^2/g. As a proof of principle, we further demonstrate that metal nanoparticles such as Pt nanoparticles, can be encapsulated into the TiO_2 shell during the digestion process and used for subsequent heterogeneous catalysis. In addition, we show that the core components of the ZIF nanocrystals, along with their adsorbed guests, can be used as precursors for the formation of secondary materials, following their thermal decomposition, to produce hollow and porous metal sulfide/titania or metal oxide/titania composite nanostructures.

INTRODUCTION

Methods for the synthesis of hollow inorganic nanostructures of metals, metal oxides, and metal sulfides have attracted much attention because of their intriguing properties and widespread applications in energy storage, drug delivery, sensing, and heterogeneous catalysis.[1−12] The size and morphology of such hollow nanostructures is typically controlled by a sacrificial template. One drawback to traditional templating methods is that template removal involves harsh treatments such as strongly acidic or basic solutions or high temperatures. This can be problematic since undesired changes to the chemical composition of the material and its structure can occur. To address these issues, fruitful and versatile methodologies involving the use of materials such as organic polymers, vesicles, and liquid droplets as soft templates have emerged.[13−16] In this context we hypothesized that small metal–organic framework (MOF) crystals could serve as useful templates for the synthesis of hollow materials. Zeolitic imidazolate frameworks (ZIFs),[17] a class of MOF constructed from tetrahedrally coordinated metal ions linked by anionic imidazolate ligands, are particularly well-suited as sacrificial templates[18] since (i) the size and shape of ZIF nanocrystals can be tuned, making a range of morphologies accessible, which would lead to hollow materials that reflect these size/shape metrics;[19] (ii) they are resistant to basic conditions but are easily decomposed in weakly acidic solution, and (iii) they exhibit excellent chemical and thermal stability.[20]

Our strategy for using ZIF crystals as soft templates is illustrated in Scheme 1. ZIF nanocrystals are first synthesized to define the shape and dimensions desired for the hollow structure. A uniform layer of a secondary material is then deposited around the ZIF crystals from soluble precursors (step (a)). This produces a ZIF@shell composite material. At this point two pathways can be followed. First, etching of the ZIF core (step (b)) using mild conditions will generate a hollow particle. Second, an additional benefit of employing ZIFs as templates may be drawn upon to produce hollow composite

Received: June 17, 2015
Published: September 14, 2015

DOI: 10.1021/acs.inorgchem.5b01352
Inorg. Chem. 2015, 54, 9483−9490

Scheme 1. Schematic Illustration of Our Strategy for Using ZIF Nanocrystals as Sacrificial Templates for the Synthesis of Hollow Structures of Other Materials with Controlled Dimensions and Morphologies

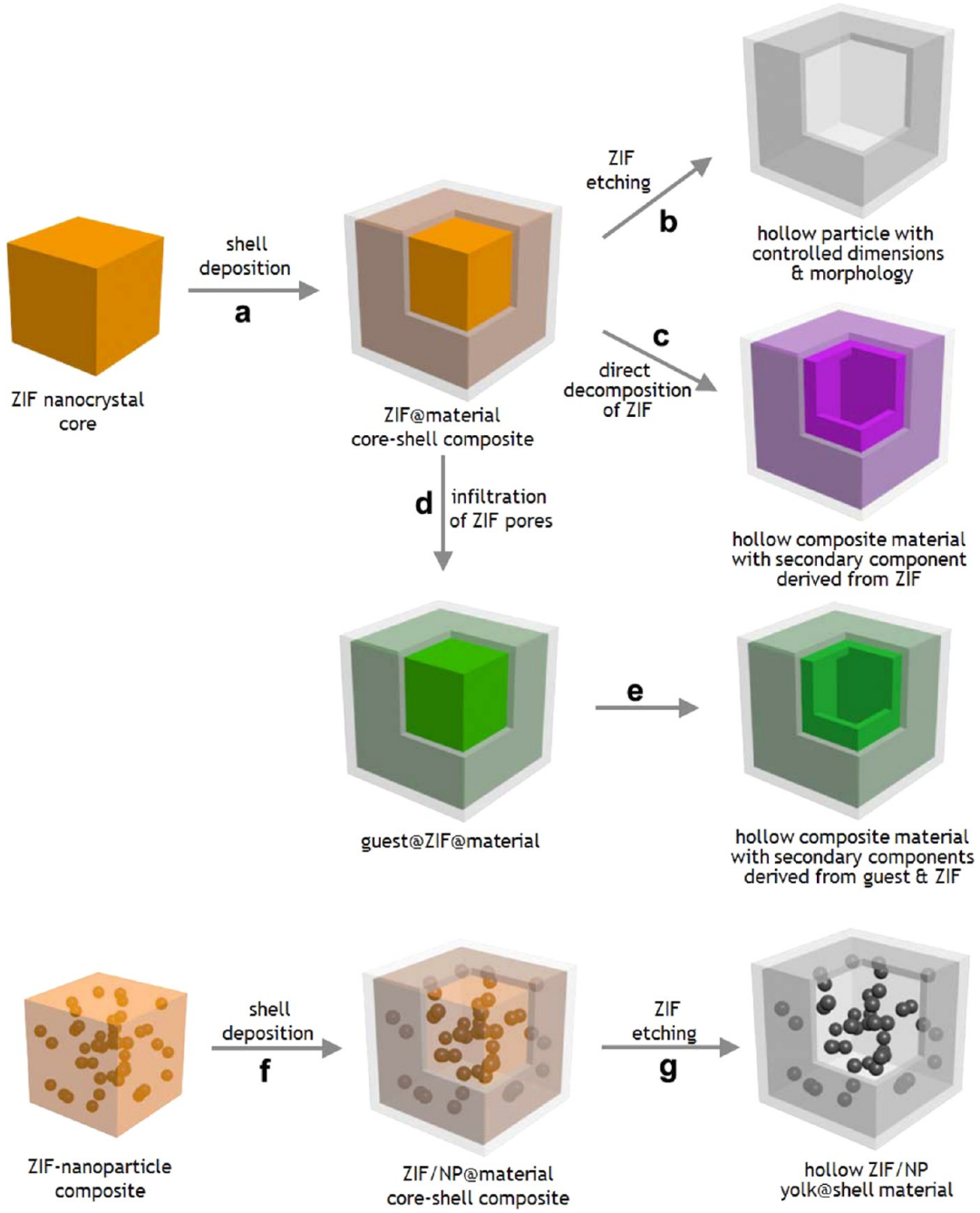

nanostructures. Here, the ZIF components are used as precursors for a secondary material (step (c)). For example, the metal component of the ZIF template could be converted into a metal oxide by oxidative pyrolysis,[21] or the ZIF can be decomposed into a carbonaceous material by anaerobic thermolysis.[22−25] A broad array of secondary materials can be deposited given the diversity of ZIFs and other MOFs. To diversify this approach to composite materials, molecular cargo can be introduced to the ZIF pores (step (d)) prior to decomposition (step (e)). We propose that an additional method for producing hollow composite materials would be to use composite ZIF nanocrystals that incorporate a secondary material such as metal nanoparticles (step (f)). Selective etching of the ZIF portion of the core will deposit the nanoparticles in the void space of the hollow material (step (g)).

We selected titania and titania-based composite materials as initial targets of the synthetic strategy outlined in Scheme 1. Titania (TiO_2) is a widely studied semiconductor material with a variety of important applications, low toxicity, high chemical stability, and wide band gap energy.[26−32] To enhance these inherent attractive properties, methods for the synthesis of hollow and/or high surface area forms of TiO_2 are highly desirable.[33−39] For instance, uniform hollow TiO_2 structures have been prepared using silica, carbon, polystyrene, and transition metal oxide particles as templates.[29,33−39] However, most of these hollow titania structures are spherical in shape. Nonspherical morphologies are much more rare due to the

DOI: 10.1021/acs.inorgchem.5b01352
Inorg. Chem. 2015, 54, 9483−9490

limited availability of suitable nonspherical sacrificial templates and problems associated with structural stability following template removal.[35] Nonspherical architectures contain higher surface-to-volume ratios than their spherical counterparts, and it is anticipated that such morphologies might be expected to have novel physicochemical properties.[40] Although appropriately shaped α-Fe_2O_3 and Cu_2O templates that lead to hollow TiO_2 ellipsoids and octahedra are known, the significant challenge of routinely creating nonspherical hollow TiO_2 structures still remains.[10] While this work was in progress aspects of this strategy were implemented by Wu et al. to produce a fascinating array of ZIF@material composites and hollow nanostructures.[40] Recently, ZIF nanocrystals have also been usefully implemented in the preparation of titania microcapsules.[41]

RESULTS AND DISCUSSION

To prepare hollow nanostructured titania using a ZIF template, cubic $[Zn(2\text{-methylimidazolate})_2]_n$ (ZIF-8) nanocrystals were first prepared via a facile synthetic route in aqueous solution at room temperature.[21,42,43] The morphologies of the ZIF nanocubes were examined by scanning electron microscopy (SEM) and transmission electron microscopy (TEM), and found to be cubic with edge lengths of 50 to 300 nm (Figure S26). Following the addition of titanium(IV) butoxide ($Ti(OBu)_4$) cubic core–shell ZIF-8@amorphous-TiO_2 composites (abbreviated as ZIF-8@am-TiO_2) were obtained after brief heating. Microscopy images clearly reveal cubic structures with an increased surface roughness (Figure S29), consistent with the successful formation of the TiO_2 shell around the ZIF-8 cubes. The thickness of the shell can be controlled by varying the concentration of the $Ti(OBu)_4$ precursor (Table 1). This is clearly observable in the microscopy images following etching of the template (vide infra). Powder X-ray diffraction (PXRD) patterns of the ZIF-8 cubes and ZIF-8@am-TiO_2 composite indicate that the ZIF core is unaltered by the deposition of the titania shell (Figure 1b,c). No additional diffraction peaks were detected for the ZIF-8@am-TiO_2 composites, which indicate that the titania shells are amorphous.

Table 1. Summary of the TiO_2 Materials Reported Herein

sample ID	template material	template shape	$Ti(OBu)_4$ added[a] (mmol)	surface area[b] ($m^2\ g^{-1}$)
am-TiO_2_1		cubic	0.73	660
am-TiO_2_2	ZIF-8	cubic	1.47	624
am-TiO_2_3		cubic	2.94	702
am-TiO_2_4		polyhedral	0.73	677
am-TiO_2_5	ZIF-8	polyhedral	1.47	731
am-TiO_2_6		polyhedral	2.94	660
am-TiO_2_7		polyhedral	0.73	725
am-TiO_2_8	ZIF-67	polyhedral	1.47	795
am-TiO_2_9		polyhedral	2.94	804
am-TiO_2_10			0.73	325
am-TiO_2_11	none		1.47	279
am-TiO_2_12			2.94	319
Pt@am-TiO_2	Pt/ZIF-8	cubic	0.25	632
TiO_2/ZnS	TA@ZIF-8@TiO_2[c]	cubic	0.73	283
TiO_2/CoS_x	TA@ZIF-67@TiO_2[c]	polyhedral	0.73	224

[a]The amount of $Ti(OBu)_4$ added during synthesis of the ZIF@am-TiO_2 core–shell materials. [b]As calculated using the BET method from a N_2 adsorption isotherm at 77 K. [c]TA = thioactetamide.

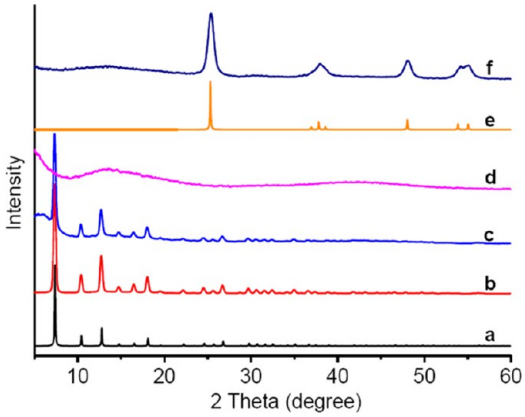

Figure 1. PXRD patterns (Cuα radiation) of (a) simulated ZIF-8; (b) as-synthesized cubic ZIF-8 nanocrystals; (c) as-synthesized ZIF-8@am-TiO_2_1 core–shell composite; (d) as-synthesized hollow am-TiO_2_1 cubes; (e) simulated anatase TiO_2; (f) as-synthesized hollow an-TiO_2_1 cubes.

Following the deposition of the TiO_2 shell around the ZIF nanocrystals, etching of the ZIF core was investigated. The experiments presented in Figure S1 show that cloudy solutions of ZIF-8 nanocrystals clarify over several seconds following the addition of dilute aqueous HCl solution. This indicates that the ZIFs decompose rapidly under these conditions, as expected. Treatment of ZIF-8@am-TiO_2 composites in a similar fashion produced hollow amorphous TiO_2 (abbreviated as am-TiO_2) cubes. There is little visible change to a suspension of ZIF-8@am-TiO_2 upon etching of the ZIF core (Figure 2a,b); however,

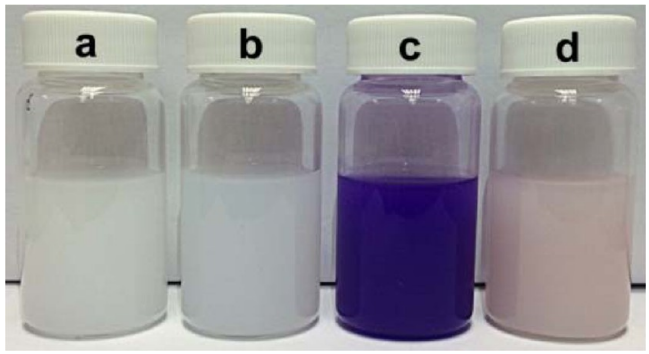

Figure 2. Photographs of aqueous solutions of (a) ZIF-8@am-TiO_2; (b) ZIF-8@am-TiO_2 after dilute HCl etching to produce am-TiO_2; (c) ZIF-67@am-TiO_2; (d) ZIF-67@am-TiO_2 after dilute HCl etching to produce am-TiO_2.

TEM (Figure 3a,b) portrays a well-defined internal void that replicates the shape of the original ZIF template. The shell thickness and roughness of hollow am-TiO_2_2 and am-TiO_2_3 cubes (Figure 3c–f) exceeds that of am-TiO_2_1 due to the additional $Ti(OBu)_4$ used in the ZIF coating step.

The hollow amorphous am-TiO_2 structures could be made crystalline without loss of their uniform shape by simply annealing in air. PXRD (Figures 1f and S9) shows that the anatase phase is produced (abbreviated as an-TiO_2). Hydrothermal heating is an alternative annealing method (Figure S18), although the PXRD peak at $2\theta \approx 18°$ may indicate a

DOI: 10.1021/acs.inorgchem.5b01352
Inorg. Chem. 2015, 54, 9483–9490

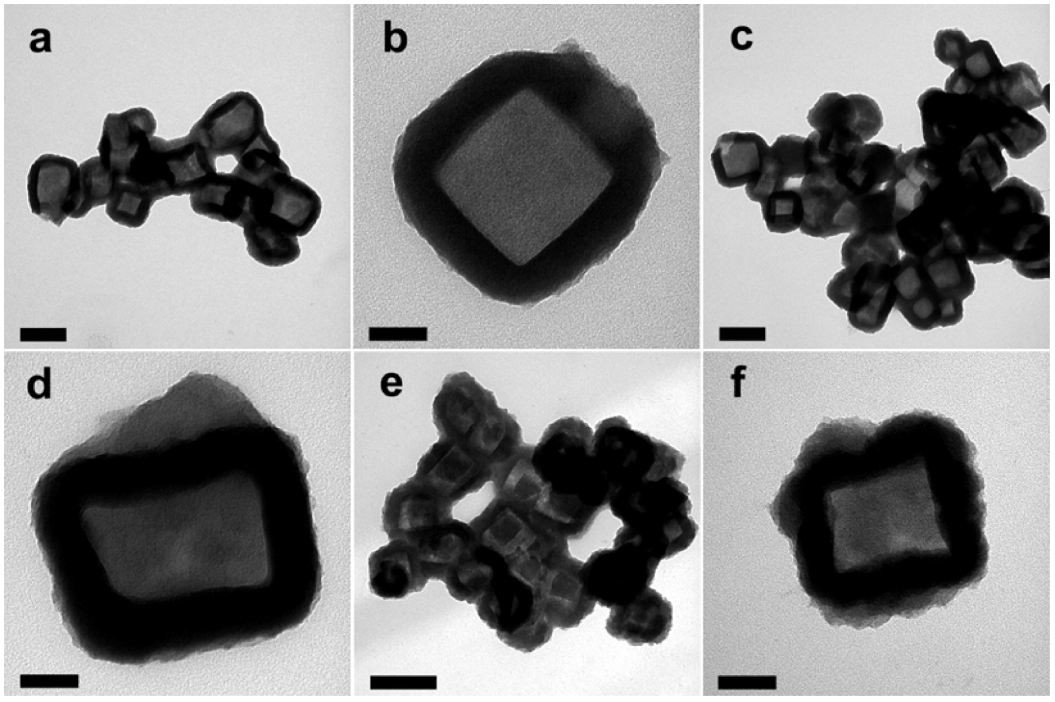

Figure 3. TEM images of (a, b) hollow am-TiO_2_1 cubes; (c, d) hollow am-TiO_2_2 cubes; (e, f) hollow am-TiO_2_3 cubes. Scale bars represent 200 nm (a, c, e) and 50 nm (b, d, f).

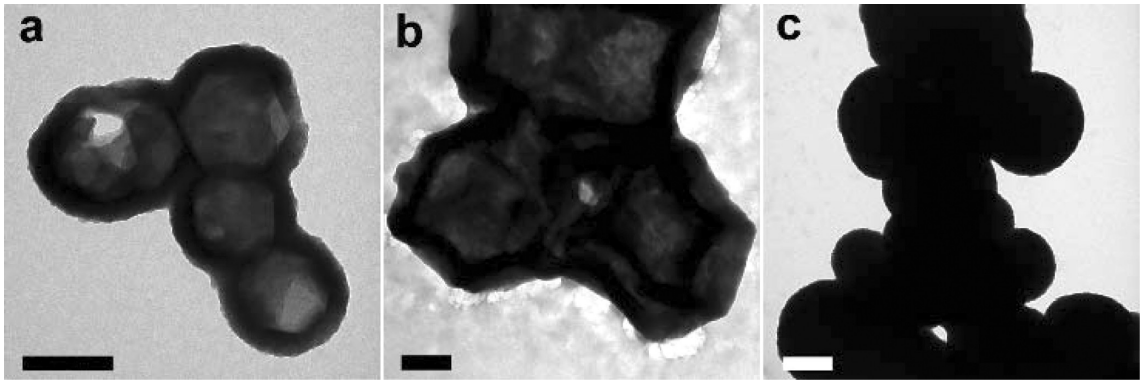

Figure 4. TEM images of (a) hollow am-TiO_2_4 polyhedra; (b) hollow am-TiO_2_7 polyhedra; (c) dense am-TiO_2_10. The scale bars represent 200 nm.

residual amorphous component. No significant variation in overall appearance or collapse of the products was observed after calcination or hydrothermal annealing, as indicated by SEM and TEM (Figures S33 and S46). However, in contrast to the am-TiO_2 structures, a significant number of small particles were observed on the surface of the cubes.

To further demonstrate the versatility of our method, hollow TiO_2 structures with polyhedral shapes were also fabricated. When polyhedral ZIF-8 nanocrystals were used for the synthesis in place of cubic nanocrystals, hollow amorphous and anatase TiO_2 structures could be produced (Table 1). Notably, the purple color of ZIF-67 disappears after HCl treatment of the ZIF-67@am-TiO_2 composite, which is consistent with etching of the ZIF core (Figure 2d). TEM (Figure 4a,b) and PXRD (Figures S11 and S14) demonstrate that the polyhedral shape of the ZIF template is replicated by the amorphous hollow TiO_2 nanoshells.

To assess the role played by the ZIF template in the fabrication of the hollow am-TiO_2 structures, we prepared TiO_2 materials in its absence (Table 1). As anticipated, hollow structures were not obtained. Instead, dense TiO_2 nanospheres were observed (Figures 4c, S42, and S43). These results point to an active role being played by the ZIF nanocrystals in promoting the deposition of the TiO_2 shells. The interior of ZIF-8 and ZIF-67 crystals are known to be strongly hydrophobic; however, their exterior surfaces are hydrophilic due to the existence of terminal hydrophilic N−H functional groups.[44] We hypothesize that in aqueous ethanolic suspensions these characteristics will favor the absorption of ethanol molecules into the ZIF pores, while H_2O molecules will preferentially coat the outer hydrophilic surface of the ZIF nanocrystals (Figure 5).[44] This would provide a high local concentration of H_2O, which may initiate hydrolysis of $Ti(OBu)_4$ on the surface of the ZIF crystals and generate partially hydrolyzed oligomers. Subsequent production of TiO_2 via a pathway involving further hydrolysis, oligomerization, and condensation into TiO_2 would deliver a uniform titania shell

DOI: 10.1021/acs.inorgchem.5b01352
Inorg. Chem. 2015, 54, 9483−9490

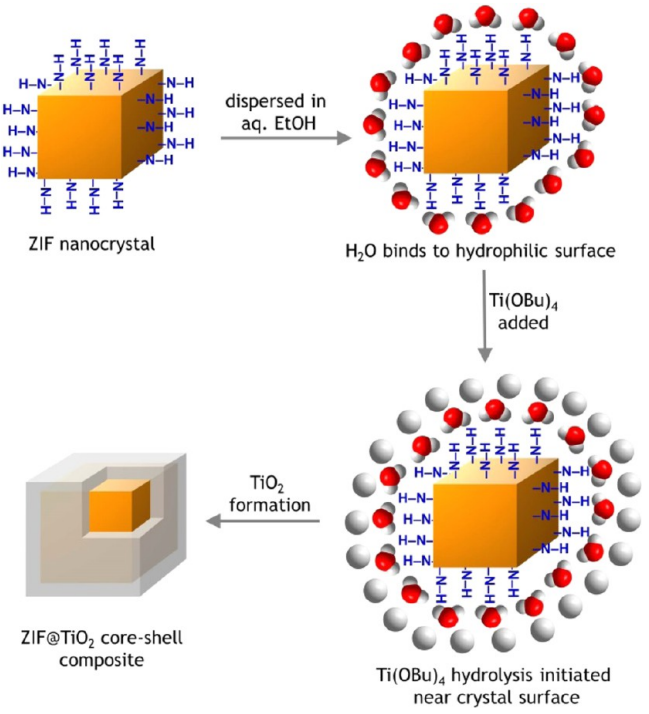

Figure 5. Schematic illustration of a plausible pathway to the ZIF-8@TiO_2 composites. Terminal N−H functional groups on the crystal surface attract water. The high local concentration of water initiates $Ti(OBu)_4$ hydrolysis titanium oligomers near the ZIF crystal surface. A uniform layer of titania is subsequently deposited to give the ZIF@TiO_2 core−shell composites.

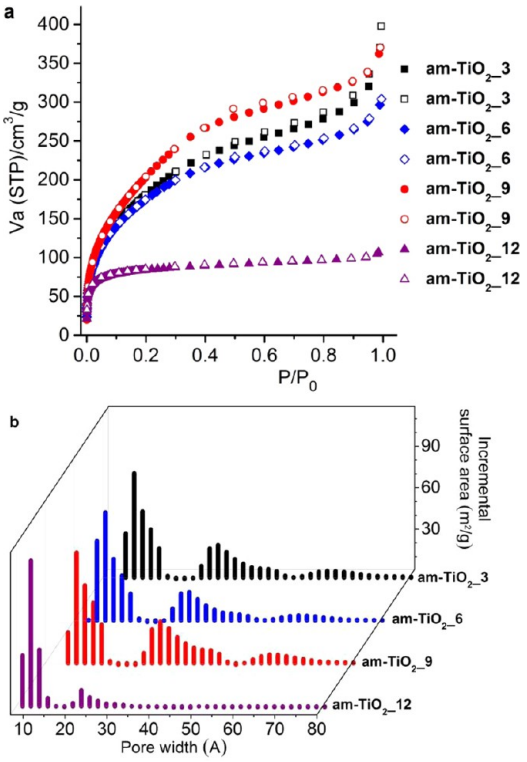

Figure 6. (a) N_2 adsorption (filled symbols) and desorption (open symbols) isotherms measured at 77 K. (b) Pore size distributions of hollow titania structures calculated from the respective N_2 adsorption isotherms using a DFT method.

that adheres to the crystal surface by Ti−O···H−N hydrogen bonds.

The textural properties of the ZIF@TiO_2 composites and hollow TiO_2 structures were assessed by N_2 adsorption experiments at 77 K. Prior to analysis, freshly prepared samples of the ZIF@TiO_2 composites and TiO_2-only materials were activated by heating under a dynamic vacuum at 80 °C for 5 h. Isotherms of the hollow TiO_2 structures were typically found to be type-II, which indicates a wide distribution of pore sizes.[45,46] For those grown using a cubic ZIF-8 template, the gravimetric adsorption capacity of the TiO_2 shells appears to correlate with the thickness of the TiO_2 shell (Figures 6 and S61). Surface areas of the TiO_2 materials calculated using the Brunauer−Emmett−Teller (BET) model range from 660 to 702 $m^2\ g^{-1}$ (Table 1). The BET surface areas of hollow TiO_2 structures produced using polyhedral ZIF-8 nanocrystals are comparable to their cubic counterparts (Table 1). In switching to ZIF-67 templates, the surface area of the TiO_2 structures increased to ~800 $m^2\ g^{-1}$. The TiO_2 spheres obtained in the absence of a ZIF template were found to be considerably less porous that the templated materials (Table 1).

The total pore volume of the amorphous TiO_2 hollow structures, calculated from their N_2 adsorption isotherms, is typically ~0.5 $cm^3\ g^{-1}$ (Table S1). The pore size distributions calculated using a density functional theory (DFT) method (Figures 6 and S75) reveal a hierarchical pore structure with void spaces in the micro-, meso-, and macropore ranges. Annealing of the hollow TiO_2 materials has a marked effect on their pore characteristics. Whereas hydrothermally annealed anatase nanoshells have relatively high BET surface areas of ~200 $m^2\ g^{-1}$ (Table S2, Figure S69), dry annealing leads reduction of the surface area to less than 100 $m^2\ g^{-1}$ (Table S2). A reduction in surface area upon annealing has previously been observed for related materials.[47,48] On the basis of the calculated pore size distributions (Figures S77−S81), the loss of accessible surface area can be mostly ascribed to the collapse of the micropores.

The surface areas and pore volumes of the amorphous TiO_2 materials prepared using ZIF templates reported herein are among the highest for reported titania materials (Table S3).[8−12,27−30,33−39,48−54] The surface areas of the anatase phases an-TiO_2_1 and an-TiO_2_7 are comparable with the best reported mesoporous anatase materials. However, we do note that the surface areas of the crystalline materials presented here may be inflated by residual amorphous titania that is hinted at by PXRD (Figure S18). These titania nanoshells are thus exciting candidates for applications as photocatalysts, catalyst supports, adsorbents, and semiconductors.

Titania is commonly used as a catalyst support due to its excellent chemical and thermal stability and its ability to disperse catalytic nanoparticles and prevent their sintering.[55] Hollow titania structures have been employed in this role. For example, nanoparticle-infused silica spheres, carbon spheres, and polystyrene spheres have been employed as templates to prepare Au@TiO_2 and Pt@TiO_2 catalysts.[56−58] We sought to implement ZIF nanocrystals as soft templates to produce related composites of hollow titania nanostructures and Pt nanoparticles (PtNPs; Scheme 1). First, small ZIF-8 nanocrystals infused with PtNPs were synthesized using a straightforward method that simply involves adding a dispersion of PtNPs to a typical ZIF-8 reaction mixture. TEM images (Figure S48) indicate that the PtNPs tend to localize near the surface of the ZIFs. Titania was deposited on

DOI: 10.1021/acs.inorgchem.5b01352
Inorg. Chem. 2015, 54, 9483−9490

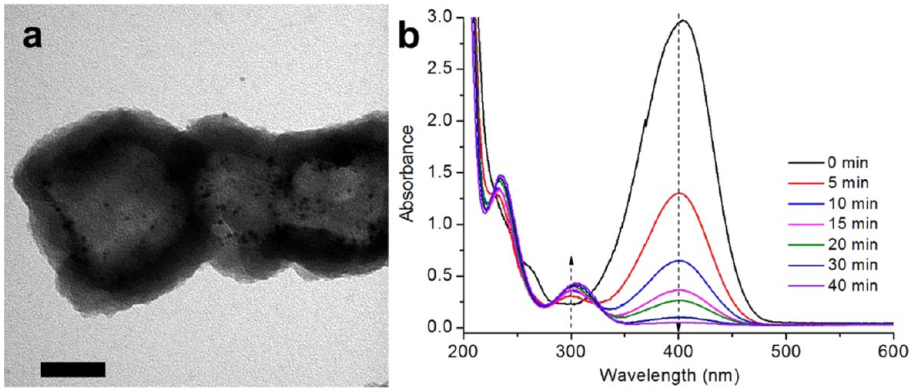

Figure 7. (a) TEM image of the Pt@am-TiO_2 composite (the scale bar represents 50 nm). The PtNPs are evident as small dark dots, and the titania appear as hollow cubes. (b) UV−visible absorption spectra for the reduction of 4-nitrophenol using Pt@am-TiO_2 as a catalyst.

the surface of the Pt/ZIF-8 nanocrystals using the methodology we had developed for the parent ZIF crystals (Figure S49) to produce Pt/ZIF-8@TiO_2 core−shell structures. The ZIF could be etched from the core of Pt/ZIF-8@TiO_2 to produce yolk−shell Pt@TiO_2 composites. Importantly, this took place without any aggregation of the PtNPs (Figure 7a). Inductively coupled plasma mass spectrometry indicated that the composite is 2.4% Pt by weight. The nitrogen adsorption isotherm of Pt@am-TiO_2 demonstrates that the high porosity of the amorphous titania support is also maintained (Figure S70) and leads to a calculated BET surface area of 632 m^2 g^{-1}.

Pt@am-TiO_2 is an ideal catalyst since it features small segregated PtNPs on a robust and porous titania support. The reduction of 4-nitrophenol by sodium borohydride, which can be conveniently monitored by UV−vis spectroscopy, was performed to assess its catalytic performance[59] The absorption peak of 4-nitrophenol at 400 nm diminishes as the reaction proceeds, and a new peak, corresponding to 4-aminophenol, appears at 300 nm (Figure 7b). We found that the reduction reaction does not proceed in absence of the Pt@TiO_2 catalyst (Figure S86). TEM images of the Pt@am-TiO_2 catalyst isolated after the catalysis reaction shows neither significant changes in the morphology of the titania nanostructures nor the aggregation state of the PtNPs (Figure S51).

Transition metal chalcogenides such as zinc sulfide and cobalt sulfide are an important class of materials that have applications as supercapacitors, lithium-ion batteries, solar cells, sensing, and catalysis.[60−63] One approach to achieving enhanced performance in these materials is to include them as components of composite materials. For example, nanostructured ZnS coupled with TiO_2, synthesized by a dipping method, exhibits excellent energy storage properties in dye-sensitized solar cells;[62] and an electrochemically fabricated TiO_2/CoS_x composite has been used in high-performance supercapacitors.[63] This inspired us to attempt the preparation of TiO_2−ZnS and TiO_2−CoS_x composite materials starting from ZIF-8@TiO_2 and ZIF-67@TiO_2. The requisite sulfur was introduced by infiltrating the ZIF pores with thioacetamide (step (d), Scheme 1). Subsequently, simple heating in ethanol/water produced solid materials with a pale yellow (ZnS/TiO_2) or black (CoS_x/TiO_2) color (Figure S2). Crucially, these composites maintained the hollow structure defined by the ZIF template (Figures 8a,b, S52, and S54). The metal sulfide component appears to deposit on the titania support as small particles. No large aggregates or clusters could be detected. Consistent with earlier observations on titania-only materials,

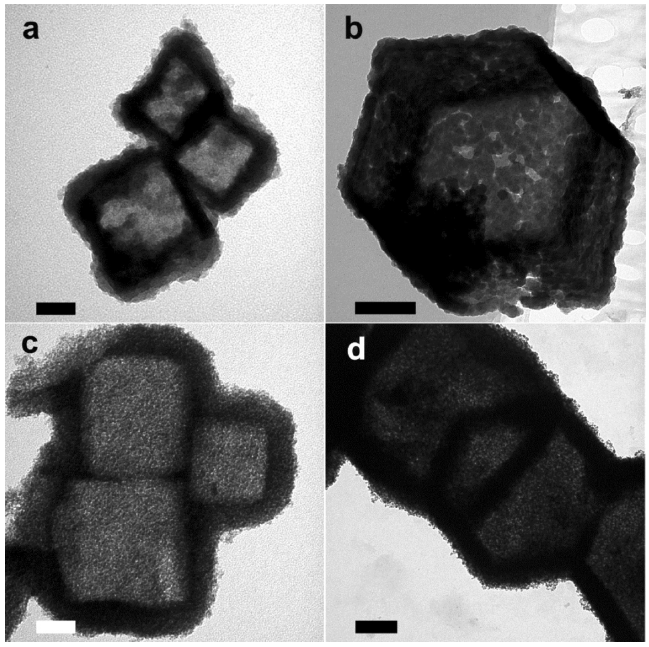

Figure 8. TEM images of (a) hollow amorphous ZnS/TiO_2; (b) hollow amorphous CoS_x/TiO_2; (c) hollow crystalline ZnS/TiO_2; (d) hollow crystalline CoS_2/TiO_2. Scale bars represent 50 nm (a, c) and 200 nm (b, d).

both the titania and metal sulfide components were amorphous at this point (Figure S21) and highly porous. The calculated BET surface areas of 283 and 224 m^2 g^{-1} (Figure S71) are lower than the titania-only materials, which may indicate that many of the titania pores become filled by the metal sulfide component. Annealing of ZnS/TiO_2 and CoS_x/TiO_2 into ZnS/an-TiO_2 and CoS_2/ an-TiO_2 by hydrothermal treatment at 180 °C produces materials that maintain their original color (Figure S3) and nanostructural features (Figures 8c,d, S53, and S55). PXRD demonstrates that, as expected, the titania component is transformed into anatase (Figures S22 and S23). The amorphous ZnS crystallizes into zinc blende (Figure S22) in ZnS/an-TiO_2, while the CoS_x evolves into cattierite (CoS_2), which has a pyrite structure, in CoS_2/an-TiO_2 (Figure S23). The BET surface areas of ZnS/an-TiO_2 and CoS_2/an-TiO_2 are estimated from N_2 adsorption isotherms at 77 K to be 139 and 156 m^2 g^{-1}, respectively (Figure S72). Pore size distribution plots derives from N_2 adsorption isotherms are presented in Figures S82−S84.

DOI: 10.1021/acs.inorgchem.5b01352
Inorg. Chem. 2015, 54, 9483−9490

To prepare hollow nanostructured composites of titania and zinc oxide or cobalt oxide we heated ZIF-8@TiO_2 cubes and ZIF-67@TiO_2 polyhedra at 550 °C under air. We observed the outer titania shell was maintained in both cases to produce hollow nanostructures (Figures S4 and S56−S59). The heating process transforms the ZIF into the corresponding metal oxide. We observed a ZnO/anatase/rutile composite in the case of ZIF-8@TiO_2 and a Co_3O_4/TiO_2 composite in the case of ZIF-67@TiO_2, as evidenced by the PXRD patterns in Figures S24 and S25.

CONCLUSION

In summary, we report a powerful method for the synthesis of well-defined, hollow materials using ZIF crystals as sacrificial templates. We have established a proof of principle by focusing on TiO_2 structures, and demonstrated that the surface of ZIF nanocrystals promotes the growth of a conformal titania coating. The ZIF core can be completely and rapidly removed without perturbing the integrity of the TiO_2 shells. The shape and dimensions of the resultant hollow TiO_2 structures are controlled by those of the sacrificial ZIF template to give rare examples of cubic and polyhedral morphologies. These titania materials exhibit exceptional textural properties. When ZIF-8 nanocrystals infused with platinum nanoparticles were employed as a template, the Pt nanoparticles were successfully encapsulated into the hollow titania cubes. The Pt@am-TiO_2 composite obtained in this way are competent catalysts for hydrogenation reactions. If the core of ZIF-titania core−shell structures is thermolyzed rather than etched, new types of hollow metal sulfide/titania and mixed metal oxide composite nanostructures can be synthesized. The present strategy is straightforward and scalable, and we expect that it will be broadly applicable to the shape- and size-controlled fabrication of hollow and porous morphologies of a wide array of other materials.

ASSOCIATED CONTENT

Supporting Information

The Supporting Information is available free of charge on the ACS Publications website at DOI: 10.1021/acs.inorgchem.5b01352.

Chemicals and instrumentation used, procedures of syntheses and annealing, tabulated pore volumes and surface areas, photographs of solutions and solid TiO_2 mixtures, PXRD patterns, SEM, TEM, and EDS images, adsorption and desorption isotherms, pore size distribution plots, UV−vis spectra of 4-nitrophenol reduction, additional references. (PDF)

AUTHOR INFORMATION

Corresponding Authors

*E-mail: s.telfer@massey.ac.nz. (S.G.T.)
*E-mail: paul.kruger@canterbury.ac.nz. (P.E.K.)
*E-mail: H.Yang2@massey.ac.nz. (H.Y.)

Author Contributions

All authors have given approval to the final version of the manuscript.

Notes

The authors declare no competing financial interest.

ACKNOWLEDGMENTS

The authors gratefully acknowledge the MacDiarmid Institute for financial support, particularly the postdoctoral fellowship to H.Y. We thank J. Taylor and N. Murray for expert assistance with the microscopy measurements, Prof. J. Pak for valuable discussions, and S. Lee for help with graphics.

REFERENCES

(1) Lou, X. W.; Archer, L. A.; Yang, Z. *Adv. Mater.* **2008**, *20*, 3987−4019.
(2) Zhao, Y.; Jiang, L. *Adv. Mater.* **2009**, *21*, 3621−3638.
(3) Hu, J.; Chen, M.; Fang, X.; Wu, L. *Chem. Soc. Rev.* **2011**, *40*, 5472−5491.
(4) Zeng, H. C. *J. Mater. Chem.* **2011**, *21*, 7511−7526.
(5) Skrabalak, S. E.; Chen, J.; Sun, Y.; Lu, X.; Au, L.; Cobley, C. M.; Xia, Y. *Acc. Chem. Res.* **2008**, *41*, 1587−1595.
(6) Nam, K. M.; Shim, J. H.; Ki, H.; Choi, S.-I.; Lee, G.; Jang, J. K.; Jo, Y.; Jung, M.-H.; Song, H.; Park, J. T. *Angew. Chem., Int. Ed.* **2008**, *47*, 9504−9508.
(7) Huang, C.; Jiang, J.; Lu, M.; Sun, L.; Meletis, E. I.; Hao, Y. *Nano Lett.* **2009**, *9*, 4297−4301.
(8) Yin, Y.; Rioux, R. M.; Erdonmez, C. K.; Hughes, S.; Somorjai, G. A.; Alivisatos, A. P. *Science* **2004**, *304*, 711−714.
(9) Hung, L.-I.; Tsung, C.-K.; Huang, W.; Yang, P. *Adv. Mater.* **2010**, *22*, 1910−1914.
(10) Wang, Z.; Zhou, L.; David Lou, X. W. *Adv. Mater.* **2012**, *24*, 1903−1911.
(11) Lai, X.; Halpert, J. E.; Wang, D. *Energy Environ. Sci.* **2012**, *5*, 5604−5618.
(12) Oh, M. H.; Yu, T.; Yu, S.-H.; Lim, B.; Ko, K.-T.; Willinger, M.-G.; Seo, D.-H.; Kim, B. H.; Cho, M. G.; Park, J.-H.; Kang, K.; Sung, Y.-E.; Pinna, N.; Hyeon, T. *Science* **2013**, *340*, 964−968.
(13) Caruso, F.; Caruso, R. A.; Möhwald, H. *Science* **1998**, *282*, 1111−1114.
(14) Xu, H.; Wang, W. *Angew. Chem., Int. Ed.* **2007**, *46*, 1489−1492.
(15) Liu, J.; Hartono, S. B.; Jin, Y. G.; Li, Z.; Lu, G. Q.; Qiao, S. Z. *J. Mater. Chem.* **2010**, *20*, 4595−4601.
(16) Zhao, Y.; Zhang, J.; Li, W.; Zhang, C.; Han, B. *Chem. Commun.* **2009**, 2365.
(17) Phan, A.; Doonan, C. J.; Uribe-Romo, F. J.; Knobler, C. B.; O'Keeffe, M.; Yaghi, O. M. *Acc. Chem. Res.* **2010**, *43*, 58−67.
(18) Ejima, H.; Yanai, N.; Best, J. P.; Sindoro, M.; Granick, S.; Caruso, F. *Adv. Mater.* **2013**, *25*, 5767−5771.
(19) Sindoro, M.; Yanai, N.; Jee, A.-Y.; Granick, S. *Acc. Chem. Res.* **2014**, *47*, 459−469.
(20) Banerjee, R.; Phan, A.; Wang, B.; Knobler, C.; Furukawa, H.; O'Keeffe, M.; Yaghi, O. M. *Science* **2008**, *319*, 939−943.
(21) Pan, Y.; Liu, Y.; Zeng, G.; Zhao, L.; Lai, Z. *Chem. Commun.* **2011**, *47*, 2071−2073.
(22) Wu, R.; Qian, X.; Zhou, K.; Wei, J.; Lou, J.; Ajayan, P. M. *ACS Nano* **2014**, *8*, 6297−6303.
(23) He, L.; Li, L.; Wang, T.; Gao, H.; Li, G.; Wu, X.; Su, Z.; Wang, C. *Dalton Transactions* **2014**, *43*, 16981−16985.
(24) Lux, L.; Williams, K.; Ma, S. *CrystEngComm* **2015**, *17*, 10−22.
(25) Tang, J.; Salunkhe, R. R.; Liu, J.; Torad, N. L.; Imura, M.; Furukawa, S.; Yamauchi, Y. *J. Am. Chem. Soc.* **2015**, *137*, 1572−1580.
(26) Fujishima, A.; Honda, K. *Nature* **1972**, *238*, 37−38.
(27) Chen, X.; Mao, S. S. *Chem. Rev.* **2007**, *107*, 2891−2959.
(28) Lu, Z.; Ye, M.; Li, N.; Zhong, W.; Yin, Y. *Angew. Chem., Int. Ed.* **2010**, *49*, 1862−1866.
(29) Lee, I.; Joo, J. B.; Yin, Y.; Zaera, F. *Angew. Chem., Int. Ed.* **2011**, *50*, 10208−10211.
(30) Gordon, T. R.; Cargnello, M.; Paik, T.; Mangolini, F.; Weber, R. T.; Fornasiero, P.; Murray, C. B. *J. Am. Chem. Soc.* **2012**, *134*, 6751−6761.
(31) Li, Y.; Sasaki, T.; Shimizu, Y.; Koshizaki, N. *J. Am. Chem. Soc.* **2008**, *130*, 14755−14762.

DOI: 10.1021/acs.inorgchem.5b01352
Inorg. Chem. 2015, 54, 9483−9490

(32) Xiong, H.; Slater, M. D.; Balasubramanian, M.; Johnson, C. S.; Rajh, T. *J. Phys. Chem. Lett.* **2011**, *2*, 2560−2565.
(33) Yang, Z.; Niu, Z.; Lu, Y.; Hu, Z.; Han, C. C. *Angew. Chem., Int. Ed.* **2003**, *42*, 1943−1945.
(34) Yang, H. G.; Zeng, H. C. *J. Phys. Chem. B* **2004**, *108*, 3492−3495.
(35) Lou, X. W.; Archer, L. A. *Adv. Mater.* **2008**, *20*, 1853−1858.
(36) Chen, J. S.; Luan, D.; Li, C. M.; Boey, F. Y. C.; Qiao, S.; Lou, X. W. *Chem. Commun.* **2009**, *46*, 8252−8254.
(37) Joo, J. B.; Zhang, Q.; Lee, I.; Dahl, M.; Zaera, F.; Yin, Y. *Adv. Funct. Mater.* **2012**, *22*, 166−174.
(38) Joo, J. B.; Lee, I.; Dahl, M.; Moon, G. D.; Zaera, F.; Yin, Y. *Adv. Funct. Mater.* **2013**, *23*, 4246−4254.
(39) Zhang, G.; Wu, H. B.; Song, T.; Paik, U.; Lou, X. W. *Angew. Chem., Int. Ed.* **2014**, *53*, 12590−12593.
(40) Wu, R.; Wang, D. P.; Han, J.; Liu, H.; Zhou, K.; Huang, Y.; Xu, R.; Wei, J.; Chen, X.; Chen, Z. *Nanoscale* **2015**, *7*, 965−974.
(41) Wang, X.; Shi, J.; Zhang, S.; Wu, H.; Jiang, Z.; Yang, C.; Wang, Y.; Tang, L.; Yan, A. *J. Mater. Chem. B* **2015**, *3*, 6587−6598.
(42) Pan, Y.; Heryadi, D.; Zhou, F.; Zhao, L.; Lestari, G.; Su, H.; Lai, Z. *CrystEngComm* **2011**, *13*, 6937−6940.
(43) Shi, Q.; Chen, Z.; Song, Z.; Li, J.; Dong, J. *Angew. Chem., Int. Ed.* **2011**, *50*, 672−675.
(44) Zhang, K.; Lively, R. P.; Zhang, C.; Koros, W. J.; Chance, R. R. *J. Phys. Chem. C* **2013**, *117*, 7214−7225.
(45) Sing, K. S. W.; Everett, D. H.; Haul, R. A. W.; Moscou, H.; Pierotti, R. A.; Rouquerol, J.; Siemieniewska, T. *Pure Appl. Chem.* **1985**, *57*, 603−619.
(46) Walton, K. S.; Snurr, R. Q. *J. Am. Chem. Soc.* **2007**, *129*, 8552−8556.
(47) Li, X.-Y.; Chen, L.-H.; Rooke, J. C.; Deng, Z.; Hu, Z.-Y.; Wang, S.-Z.; Wang, L.; Li, Y.; Krief, A.; Su, B.-L. *J. Colloid Interface Sci.* **2013**, *394*, 252−262.
(48) Li, X.-Y.; Chen, L.-H.; Li, Y.; Rooke, J. C.; Wang, C.; Lu, Y.; Krief, A.; Yang, X.-Y.; Su, B.-L. *J. Colloid Interface Sci.* **2012**, *368*, 128−138.
(49) Yun, H. J.; Lee, H.; Joo, J. B.; Kim, W.; Yi, J. *J. Phys. Chem. C* **2009**, *113*, 3050−3055.
(50) Zhang, J.; Bang, J. H.; Tang, C.; Kamat, P. V. *ACS Nano* **2010**, *4*, 387−395.
(51) Maeda, K.; Domen, K. *J. Phys. Chem. Lett.* **2010**, *1*, 2655−2661.
(52) Ren, T.-Z.; Yuan, Z.-Y.; Su, B.-L. *Chem. Phys. Lett.* **2003**, *374*, 170−175.
(53) Fattakhova-Rohlfing, D.; Zaleska, A.; Bein, T. *Chem. Rev.* **2014**, *114*, 9487−9558.
(54) Hu, X.; Skadtchenko, B. O.; Trudeau, M.; Antonelli, D. M. *J. Am. Chem. Soc.* **2006**, *128*, 11740−11741.
(55) Sang, L.; Zhao, Y.; Burda, C. *Chem. Rev.* **2014**, *114*, 9283−9318.
(56) Lee, I.; Joo, J. B.; Yin, Y.; Zaera, F. *Angew. Chem., Int. Ed.* **2011**, *50*, 10208−10211.
(57) Ngaw, C. K.; Xu, Q.; Tan, T. T. Y.; Hu, P.; Cao, S.; Loo, J. S. C. *Chem. Eng. J. (Amsterdam, Neth.)* **2014**, *257*, 112−121.
(58) Aoi, Y.; Kambayashi, H.; Kamijo, E.; Deki, S. *J. Mater. Res.* **2003**, *18*, 2832−2836.
(59) Lu, Y.; Mei, Y.; Drechsler, M.; Ballauff, M. *Angew. Chem., Int. Ed.* **2006**, *45*, 813−816.
(60) Yu, X.; Yu, J.; Cheng, B.; Huang, B. *Chem. - Eur. J.* **2009**, *15*, 6731−6739.
(61) Jiang, Z.; Lu, W.; Li, Z.; Ho, K. H.; Li, X.; Jiao, X.; Chen, D. *J. Mater. Chem. A* **2014**, *2*, 8603−8606.
(62) Srinivasa Rao, S.; Punnoose, D.; Venkata Tulasivarma, C.; Pavan Kumar, C. H. S. S.; Gopi, C. V. V. M.; Kim, S.-K.; Kim, H.-J. *Dalton Transactions* **2015**, *44*, 2447−2455.
(63) Ray, R. S.; Sarma, B.; Jurovitzki, A. L.; Misra, M. *Chem. Eng. J. (Amsterdam, Neth.)* **2015**, *260*, 671−683.

DOI: 10.1021/acs.inorgchem.5b01352
Inorg. Chem. 2015, 54, 9483−9490